Nanoscience and Nanotechnology Letters
Vol. 3, 763–768, 2011

Numerical Study on Mechanism of Nanoparticle Formation in High Temperature Reactor

Oluranti Sadiku* and Emmanuel Rotimi Sadiku

Department of Mechanical Engineering, Faculty of Engineering and the Built Environment, Tshwane University of Technology, Private Bag x025 Lynnwoodridge 0040, Republic of South Africa

Properties of nanoparticles are size-dependent, therefore nucleation and growth of particle is often difficult. The population balance model has been developed to study the mechanism of nanoparticles formation in high temperature reactor. Processes responsible for particle formation and growth are considered by homogeneous nucleation, condensation and Brownian coagulation. Parameters such as temperature, residence time and reactant concentrations influencing particle size are investigated. The population balance model is the dynamic model that describes the evolution of the aerosol size distribution with time. The method of moments was used to solve the dynamic equation under the assumption of log-normal size distribution. The model was validated with existing model.

Keywords: Nanoparticles, Modelling, Population Balance Equation, Method of Moments, Log-Normal Size Distribution, Particle Formation, Nucleation and Coagulation.

1. INTRODUCTION

A topic area that moves increasingly into the area of nanotechnology is the formation and the production of nanoparticles in gaseous phase reactions. Nanosized (i.e., smaller than tens of nanometers) particles often behave differently, both physically and chemically, than their larger counterparts. Nanoparticles are of great scientific interest as they are effectively a bridge between bulk materials and atomic or molecular structures. Thus, in recent years, resulting from the advancement in materials synthesis, it has been possible to embed nanoparticles with controlled size in bulk materials. Zabarjadi et al.[1] The properties of materials change as their size approaches the nanoscale level. Particles with diameters in the range of 1–100 nm are of great interest for the fabrication of advanced high–performance materials. Aerosol processes have potential advantages for the production of nanoparticles with high yields and providing a molecular mixing for composite nanoparticle materials, Lixi et al.[2] Although a number of gas-phase synthesis processes exist, they all have in common, the fundamental aspects of particle formation mechanisms that occur once the product species is generated. The product quality and application characteristics of nanostructured materials depend strongly on the size distribution, morphology and the state of aggregation, i.e., the size and number of primary particles defining the degree of aggregation. In gas-phase reactors, the final product characteristics are determined by fluid mechanics and particle dynamics within a few milliseconds at the early stages of the synthesis process. Within this short time frame, there are three major formation mechanisms which dominate particle formation. The chemical reaction of the precursor leads to the formation of product monomers (clusters) by nucleation and to the growth of particles via the reaction of precursor molecules on the surface of the newly formed particles. An essential mechanism which inevitably occurs at high particle concentrations and in all industrial aerosol processes is the coagulation process.

Numerous experimental studies have suggested that aerosol growth occurs in stages, beginning with the gas phase chemical reaction of the reactants, to produce monomers or molecules of the condensable species. Christofides.[3] The monomers form unstable clusters, which grow further by monomer condensation. Beyond a critical cluster size, nucleation of stable aerosol particles occurs. These particles grow further; mainly by coagulation (condensation and surface reaction are some other growth mechanisms). The coagulation rate which is affected additively by Brownian and turbulent shear forces has a strong effect on particle size and morphology. The dynamic model of aerosol processes is typically obtained from the application of population, material and energy balances, and consists of nonlinear partial integro—differential equation systems. The complex nature of aerosol process models has motivated an

*Author to whom correspondence should be addressed.

extensive research activity on the development of numerical methods for the accurate computation of their solution. The following are examples of solution methods.

The sectional approach[4] is conceptually straightforward and offers more degrees of freedom, ensuring greater generality. The sectional method may be computationally very demanding because its accuracy is directly related with the number of discretization sections (size bins) that are used. Gelbard et al.[4] observed that numerical solutions for dynamic aerosol balances require approximation of the continuous size distribution by some finite set of classes or sections. Debra and Sonia[5] described a single moment sectional model to simulate the evolution of an aerosol distribution that contains more than one chemical component. The proposed method is based on dividing the particle domain into X sections with time variant sections boundaries.

To alleviate the problem with numerical diffusion in the presence of the surface growth, Kumar and Ramakrishna,[6–8] introduced a pivot technique combined with a moving grid and also the method of characteristics. Vanni[9] coupled a sectional model to a detailed gas phase mechanism to calculate the soot particle size distribution in a continuous stirred tank reactor (CSTR). Kalani and Christofides[10] used the sectional model to divide the continuous particle size distribution (PSD) into a finite number of sections within which the size distribution function is assumed to be constant. Suddah and Mark[11] used the sectional method of moment to approximate the continuous size distribution by a finite number of sections or bins within which one numerically conserved aerosol property is held constant.

The finite element method is a numerical technique which gives approximate solutions to differential equations to problems arising in physics and engineering.[12] In the finite element approach, the solution of the population balance is expanded in series of polynomials. James and Panagiotis,[13] proposed a finite-dimensional approximation and control of nonlinear parabolic partial differential equation (PDE) systems by combining Galerkin's method with the concept of approximate initial manifolds. Aleck and Costas[14] used orthogonal collection of finite element methods to solve a continuous form of general population balance equation (PBE). Hailian, Fraser and Martin[15] developed a predictive controller for parabolic convection–diffusion–reaction systems operating in convection-dominated regimes. Dan et al.,[16] designed a control algorithm on the basis of finite dimensional models to capture the dominant dynamics of particulate processes.

Monte Carlo (MC) methods are easy to implement, can account for fluctuations, and can easily incorporate several internal coordinates. In the case of nanoparticle modeling, the number of particles is so large that the fluctuations in particle numbers can be neglected. One of the applications of Monte Carlo methods is the stochastic Monte Carlo (MC) method which is based on the principle that the dynamic evolution of an extremely large population of particles, *Np(t)*, can be followed by tracking down the relevant particle events (i.e., growth, aggregation, nucleation). Meimaroglou, Roussos and Kiparissides[17] used this method. The kinetic Monte Carlo (KMC) method is used to estimate and control methodologies for surface properties (e.g., surface roughness). Dan et al.,[16] developed Kinetic Monte-Carlo simulators of a surface based on small lattice size models to capture the dominant roughness evolution and utilize the available surface roughness measurements to improve upon the predictions of the kinetic Monte-Carlo simulators in order to obtain accurate surface roughness estimates.

The least squares method (LSM) is a well-established technique for solving a wide range of mathematical problems. The basic idea in the LSM is to minimize the integral of the square of the residual over the computational domain, in the case when the exact solutions are sufficiently smooth the convergence rate is exponential. Daora and Jakobosen,[18] applied the least square method to solve the population balance equation.

The method of moments (MOM) is computationally the most efficient approach to obtain a numerical approximation to the moments of population balance. For this reason, this method is often used when simulating problems where transport of particles in a flow with complex geometry is essential. Dorao and Jakobson[19] derived quadrature method of moments (QMOM) in two ways, i.e., the standard quadrature method of moments which is a numerical closure for method of moments (MOM) and the method of moments in the method of weighted residuals (MOM-MWR). The second technique is the method of moment with internal closure (MOMIC). Diemer and Ehrman[20] developed a design for the comparison of reconstructed distributions from moment with direct calculation via sectional method. Barret and Webb[21] compared some approximation methods for solving the aerosol dynamic equation.

1.1. High Temperature Reactor Technologies

Nanoparticle synthesized in high temperature reactor often carries certain charges, which can be further utilized in the electrostatic manipulation, measurement and control of such particles. The nanoparticles produced at high temperature usually undergo rapid coalescence, with complex rate laws. "High-temperature methods based on flames or thermal plasma are often used for ultrafine (nanoscaled) powder synthesis. The main processes in these methods are the raw substance vapourization and the vapour-phase condensation that follows it. The condition under which the condensation takes place has an important impact on particle growth process.[22] Moropeng and Kolesnikov used one dimensional model to develop a cooled reactor-wall in order to predict the aerosol formation, growth and thermophoretic deposition in high temperature reactor.[23] The

different physical and chemical properties of nanoparticles are as a result of two basic phenomena: the surface area which results from the formation of the product molecules and clusters. These entities grow to nanoparticles by collision and sintering mechanisms at temperatures up to 3000 °C. A specific particle size for the deviation from the microscopic behavior cannot be defined, since it depends on the material, the process temperature and pressure. There is a need for detailed understanding of nanoparticle formation especially, the material synthesis and combustion in high temperature processes. The objective of this study is to develop a mathematical model for mechanism of nanoparticle formation, as it could reveal the optimum process condition for particle formation with desired properties.

2. PROCESS DESCRIPTION

Nanoparticle growth in chemical reactors is often the result of the heterogeneous reaction rather than 'physical condensation.' Titanium dioxide (TiO_2) particles are important in our daily lives. Titanium dioxide (TiO_2) nano-particles are traditionally used as pigments, but have found use in diverse areas like photocalalysis and in reducing nitrogen oxide emissions. The premixed and preheated reactants (titanium tetrachloride and oxygen gas) are injected into the reactor where the following exothermic reaction (see Eq. (1) below) takes place. The products of these reactions are titania monomers and chlorine gas. The size of a single TiO_2 molecule (monomer) is larger than the thermodynamic critical cluster size. As a result, the difference between chemical reaction and nucleation cannot be noticed, thereby implying that the rapid chemical reaction leads to nucleation burst, Sadiku and Kolesnikov.[24] The coagulation of TiO_2 monomers leads to an increase in the average particle size and a decrease in particle concentration.

$$\mathrm{TiCl_4(g) + O_2(g) \rightarrow TiO_2(nanoparticles) + 2Cl_2(g)} \quad (1)$$

2.1. Population Balance Model

The population balance equation that consists of nonlinear partial integro-differential equation is given below:

$$\frac{\partial n}{\partial t} + \frac{\partial (G(v, \bar{x})n)}{\partial v} - I(v^*)\delta(v - v^*) = \frac{1}{2}\int_o^v \beta(\tilde{v}, v-\tilde{v}, \bar{x}) n(\tilde{v}, t) n(v-\tilde{v}, t) d\tilde{v} - n(v, t) \times \int_o^\infty \beta(v, \tilde{v}, \bar{x}) n(\tilde{v}, t) d\tilde{v} \quad (2)$$

The first term on the left hand side of Eq. (2) describe the change in the number concentration of particle volume interval v, $v + dv$, $n(v, t)$ denotes the particle size distribution function, v is particle volume, t is time, the third term on the left hand side accounts for the formation of new particles of critical volume v^* by nucleation rate I. $I(v^*)\delta(v - v^*)$, and it also accounts for gain and loss of particles by condensation. The second term on the left hand side gives the loss or gain of particles by condensational growth. $I(v^*)$ and $\beta(\tilde{v}, v - \tilde{v}, \tilde{x})$ are the nonlinear scalar functions and δ is the standard Dirac function.

The mass and energy balance model which predicts the spatio-temporal evolution of the concentrations of species and temperature of the gas phase given by Kalani and Christofides[10] has the following form:

$$\frac{d\bar{x}}{dt} = \bar{f}(\bar{x}) + \bar{g}(\bar{x})u(t) + \bar{A}\int_0^\infty a(\eta, v, x) dv \quad (3)$$

where $\bar{x}(t)$ is an n-dimensional vector of state variables that depends on space and time, $\bar{A}$ is constant matrix, $\bar{f}(\bar{x})$, $\bar{g}(\bar{x})$, $a(\eta, v, x)$ are nonlinear vector functions, $u(t)$ is the time varying manipulated input (e.g., wall temperatures, Tw_1 and Tw_2). The term $\bar{A}\int_0^\infty a(\eta, v, x) dv$ accounts for mass and heat transfer from the continuous phase to all the particles in the population. The gain and loss of particles by Brownian coagulation is described by the first and second term on the right hand side of Eq. (2) respectively.

$G(v, \bar{x})$and β are the condensational growth and collision frequency function, respectively for which two different expressions are used for free molecule size and continuum size regimes.[10] The free molecule size regime takes the following form:

$$G_{\mathrm{FM}}(\bar{x}, v, z) = B_1 v^{1/3}(S - 1), \quad \text{where } B_1 = (36\pi)^{1/3} v_1 n_{\mathrm{s}} (k_{\mathrm{B}} T / 2\pi m_1)^{1/2}$$

$$\beta_{\mathrm{FM}}(\bar{x}, v, z) = B_2 \left(\frac{1}{v} + \frac{1}{v}\right)^{1/2} (v^{1/3} + \bar{v}^{1/3})^2, \quad B_2 = (3/4\pi)^{1/6} (6 k_{\mathrm{B}} T v_1 / m_1)^{1/2} \quad (4)$$

And the continuum size regime takes the following form:

$$G_C(\bar{x}, v, z) = B_3 v^{1/3}(S - 1), \quad \text{where } B_3 = (48\pi^2)^{1/3} D v_1 n_{\mathrm{s}}, \quad D = \lambda (8 k_{\mathrm{B}} T / \pi m_1)^{1/2} / 3,$$

$$\beta_C = B_4 \left(\frac{C(v)}{v^{1/3}} + \frac{C(\bar{v})}{\bar{v}^{1/3}}\right)(v^{1/3} + \bar{v}^{1/3}), \quad B_4 = \frac{2 k_{\mathrm{B}} T}{3\mu}. \quad (5)$$

In Eqs. (4) and (5), T is the temperature, S is the saturation ratio, D is the condensable vapour diffusivity, λ is the mean free path of the gas, μ is the fluid viscosity, n_{s} is the monomer concentration at saturation. ($n_{\mathrm{s}} = P_{\mathrm{s}}/k_{\mathrm{B}}T$, where P_{s} is the saturation pressure), m_1 is the monomer mass, v_1 is the monomer volume, r is the particle radius, $C(v) = 1 + B_5 \lambda / r$ is the Cunningham correction factor and B_5 = 1.257. Lastly, the nucleation rate $I(v^*)$ is assumed

to follow the classical Becker-Doring theory given by the expression below (Pratsinis).[25]

$$I = n_s^2 s_1 (k_B T/2\pi m_1)^{1/2} S^2 (2/9\pi)^{1/3} \sum^{1/2} \exp(-k^* \mathrm{In} S/2) \quad (6)$$

where s_1 is the monomer surface area and k^* is the number of monomer in critical nucleus and is given by:

$$k^* = \frac{\pi}{6}\left(\frac{4\sum}{InS}\right)^3 \quad (7)$$

where $\sum = \gamma v_1^{2/3}/k_B T$ and γ is the surface tension.

3. LOGNORMAL AEROSOL SIZE DISTRIBUTION

The population balance model in Eq. (2) is highly complex and does not allow the direct use for numerical computation of the size distribution in real-time. To overcome this problem and to accelerate the computations, method of moments was employed to solve the population balance model. In order to describe the spatio-temporal evolution of the three leading moments of the volume distribution (which describes the exact evolution of the lognormal aerosol size), a lognormal function was employed in moment model, which was applied to population balance model.

3.1. Moment Model

We assumed that the aerosol size distribution can be adequately represented by lognormal function which is described as:

$$n(v,t) = \frac{1}{3v}\frac{1}{\sqrt{2\pi}\mathrm{In}\sigma}\exp\left[-\frac{\mathrm{In}^2(v/v_g)}{18\mathrm{In}^2\sigma}\right] \quad (8)$$

where v_g, is the geometric average particle volume and σ is the standard deviation. The kth moment of the distribution is defined as:

$$M_k(t) = \int_0^\infty v^k n(v,z,t)dv \quad (9)$$

Table I. Dimensionless variables by Ashish and Panagiotis.

$N = M_0/n_s$, $V = M_1/n_s v_1$	Aerosol concentration and volume
$V_2 = M_2/n_s v_1^2$	Second aerosol moment
$\tau = (2\pi m_1/k_B T)^{1/2} n_s s_1$	Characteristic time for particle growth
$K = (2k_B T/3\mu)n_s\tau$, $I' = I/(n_s/\tau)$	Coagulation coefficient and Nucleation rate
$K_{n_1} = \lambda/r_1$	Knudsen number
$v_g' = v_g/v_1$, $r_g' = r_g/r_1$	Geometric volume and geometric radius
$\bar{z} = z/L$	Dimensionless distance
$c_{zl} = \tau c_z/L$, $\theta = t/\tau$	Dimensionless velocity and time

Source: Reprinted with permission from [26], A. Kalani and P. D. Christofides, *Chem. Eng. Sci.* 54, 2669 (**1999**). © 1999, Elsevier.

Table II. Process model parameters for the simulation study.

$D = 0.1$ m	Reactor diameter
$P_0 = 101000$ pa	Process pressure
$T_0 = 4500$ K	Inlet temperature
$T_w = 300$ K	Wall temperatures
$y_{10} = 0.5$	Inlet mole fraction of O_2 reactant
$y_{10} = 0.5$	Inlet mole fraction of $TiCl_4$ reactant
$U = 160$ Jm^{-2} s^{-1} K^{-1}	Overall coefficient of heat transfer
$\Delta H_R = 88000\ J$ mol^{-1}	Heat of reaction
$Cp = 1615.25$ mol^{-1} K^{-1}	Heat capacity of process fluid
$MW_g = 14.0 \times 10^{-3}$ kg mol^{-1}	Mol wt. of process fluid
$K = 11.4$ m^3 mol^{-1}s^{-1}	Reaction rate constant
$\mu = 6.7 \times 10^{-5}$ kg m^{-1} s^{-1}	Viscosity of process fluid
$Ps = \exp(-4644/T + 0.906^* \log(T) - 0.00162^* T + 9.004)^* (101000/760)$ Pa	Saturation pressure
$\gamma = 0.08$ N m^{-1}	Surface tension
$v_1 = 5.33 \times 10^{-29}$ m^3	Monomer volume
$N_{av} = 6.023 \times 10^{23}$# mol^{-1}	Avogadro's constant
$R = 8.314$ J mol^{-1} K^{-1}	Universal gas constant
$k_B = 1.38 \times 10^{-23} J$ K^{-1}	Boltzmann's constant
$so = 1.1587E - 19$	Surface area of monomers
$\sigma = 0.5$	Sigma

According to the properties of a lognormal function, any moment can be written in terms of M_0, v_g, and σ as follows:

$$M_k = M_0 v_g^k \exp\left(\frac{9}{2}k^2 \mathrm{In}^2\sigma\right) \quad (10)$$

If Eq. (11) is written for $k = 0$, 1, and 2, then v_g and σ can exactly be expressed in terms of the first three moments of the distribution according to the following relations:

$$\mathrm{In}^2\sigma = \frac{1}{9}\mathrm{In}\left(\frac{M_0 M_2}{M_1^2}\right), \quad v_g = \frac{M_1^2}{M_0^{3/2} M_2^{1/2}} \quad (11)$$

Tables I and II gives the dimensionless variable and process parameters used in the simulation.

4. ANALYSIS OF OPEN LOOP SIMULATION AND DISCUSSION

The process parameters used for the open loop simulation is given in Table II. Once a sufficiently high super saturation is achieved as result of condensable species, nucleation occurs. After nucleation, particle growth can be produced in two different ways: via condensation or coagulation. The growth of nucleated particles occurs by two simultaneously acting mechanisms: Particle-monomer collisions and particle-particle collisions. The former mechanism governs the first stages of coagulation; the latter mechanism is the only possible mechanism that takes place once monomers have been completely consumed in the gas phase. Typically, increasing temperature, reactor residence time and reactant concentration result in larger TiO_2 particles, but the spread of particle size distribution is not affected, indicating that particle growth takes place by coagulation. Figure 1 shows the steady state profile of

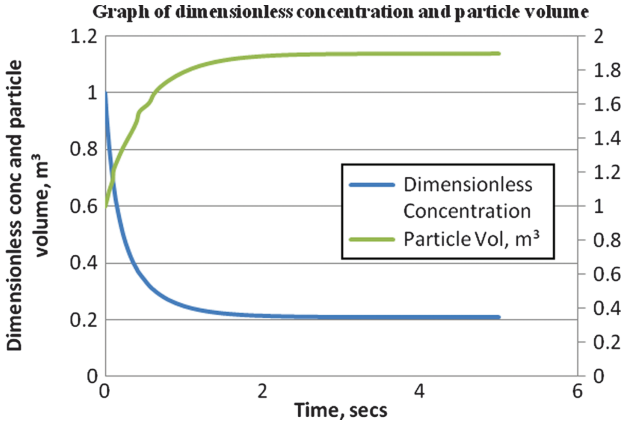

Fig. 1. Steady state profile of dimensionless number concentration and particle volume as function of time.

dimensionless particle number concentration, N and particle volume v as a function of time. The result shows continuous decrease in number concentration due to coagulation and this coagulation is caused by relative motion among particles. The decrease is also as a result of collisions due to Brownian collisions. As particles collide they grow in size thereby increasing the particle volume. The mechanism of number concentration determines the size of aerosol particles. The total surface area also increases due to coagulation as shown in Figure 2. The same graph of Figure 2 shows the distribution of particle diameter with process time. Particle diameter in the reactor increases with increasing process time. It can be seen from Figure 2 that when particles are nucleated, a primary particle and the frequency of bi-particle collision increases, resulting in an increase in the particle diameter.

Both coagulation and condensation cause particle to grow in size, increasing the particle volume.

Figure 3 shows the variation of saturated vapour pressure with the process temperature. Initially, an increase in the process temperature increases the average energy of the

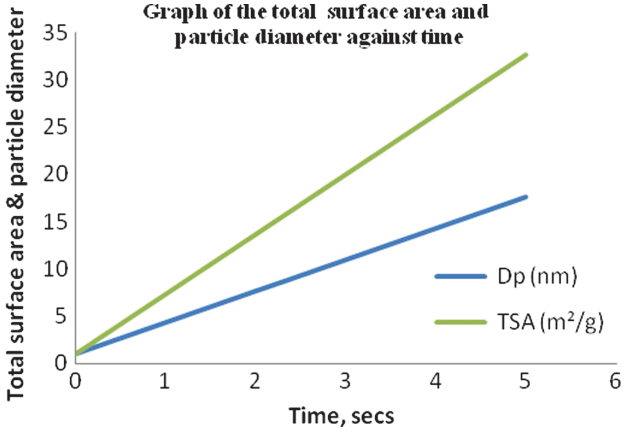

Fig. 2. The steady state profile of total surface area, (m^2/g) and the average particle diameter (nm) against the time, (secs). The total surface area increases due to collision and coagulation.

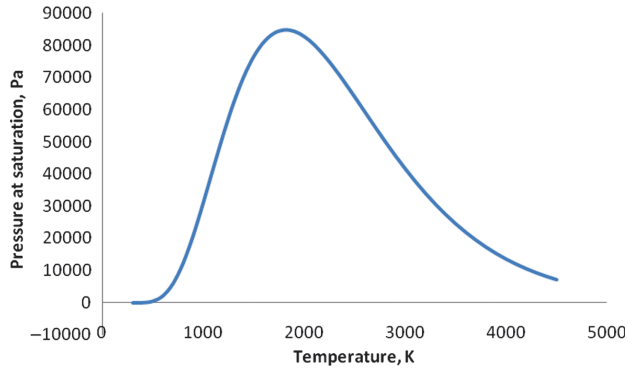

Fig. 3. The variations of saturation vapour pressure with the process temperature.

particles in the reactor which, in turns, increases the saturated vapour pressure. At some point, the gradual increase in the temperature dependence on particles decreases the saturated vapour pressure due to high force of attraction as shown in Figure 3.

Figure 4 shows the reduction of titanium tetrachloride and oxygen concentration due to combustion. The energy released and the heat evolved when $TiCl_4$ is burned in O_2 was sufficient for the chemical reaction to take place and thus resulted to the consumption of the concentration of titanium tetrachloride and oxygen. It is important to know that for successful oxidation, it is necessary to bring the reacting gases together at suitable temperature in order to provide suitable nuclei on which the particles may be formed.

5. SUMMARY

The mechanism of nanoparticle formation in high temperature reactor was studied by Modeling. The mathematical model relating the characteristics of the product powder (size and surface area) to the process variables (reactant composition, residence time and temperature) gives a very sound understanding of particle formation and growth and can thus be used to optimize the process parameters. The results obtained from this model can identify the roles each parameter played in the definition of nanoparticles formation. Among these parameters, residence time, reactant concentration of O_2, $TiCl_4$ and process temperature are of the most important, because they directly affect the final size of particles. Under high temperature reactor, the total surface area and the average particle diameter increases with increasing residence time. The final particle size at high temperature is caused by the process of particle–particle coagulation rates. The inclusion of the fractal character of colliding particles leads to significant improvement when compared with models that only considered coalescence. However, the modeling approach used within the frame of this work, can also be applied to simulate synthesis and growth of various other materials, such as Al_2O_3 or SiO_2, provided the required data of materials

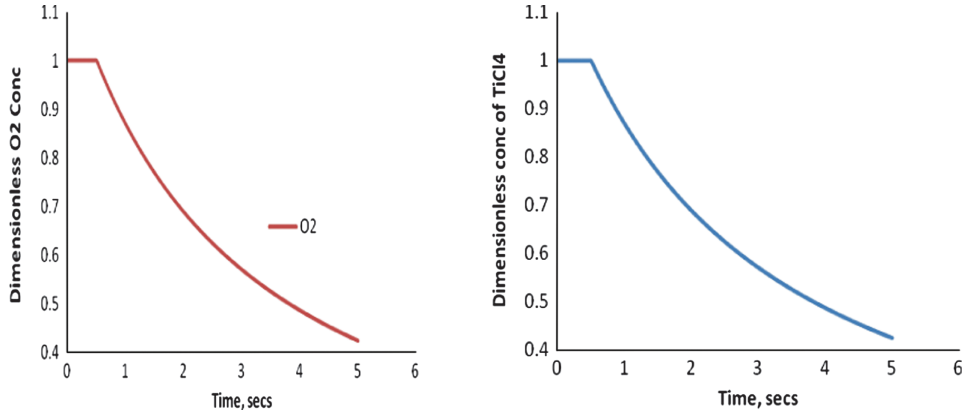

Fig. 4. The dimensionless concentration of O_2 and $Ticl_4$ as function of time.

are available. The model presented in this study helps to get a detailed view of particle formation and growth with respect to the evolution of particle characteristics; such as particle number concentration, shape and particle size which make up the product value and it can be used for optimum operation and performance of nanoparticle process with desired properties. The model was validated with existing models.

6. CONCLUSION

The product quality was influenced by a sensible selection of the process parameters. However, linking process parameters such as temperature, reactant concentration and residence time to product characteristics, requires a good understanding of the physico-chemical fundamentals of gas-phase synthesis. Therefore, process simulation is a useful tool and can significantly improve the general understanding of particle formation and moreover it can support product and process optimization. Based on the numerical study of the understanding of nanoparticle formation mechanism, it is possible to precisely optimize the process under high temperature since it produced the desired particle size.

References and Notes

1. M. Zabarjadi, K. Esfarjani, A. Shakori, Z. Bian, J. Bahk, G. Zeng, J. Bowers, H. Lu, J. Zide, and A. Gossard, *J. Electron. Mater.* 38, 954 **(2009)**.
2. W. Lixi, C. Si, and X. Hongyong, *China Particuology* 2, 215 **(2004)**.
3. P. D. Christofides, Model Based Control of Particulate Processes, Springer, New York **(2002)**.
4. F. Gelbard, Y. Tambour, and J. H. Seinfeld, *J. Colloid Interface Sci.* 76, 536 **(1980)**.
5. Y. H. Debra and M. K. Sonia, *Journal of Atmospheric Environment* 32, 1701 **(1998)**.
6. S. Kumar and D. Ramkrishna, *Chem. Eng. Sci.* 51, 1311 **(1996)**.
7. S. Kumar and D. Ramkrishna, *Chem. Eng. Sci.* 51, 1333 **(1996)**.
8. S. Kumar and D. Ramkrishna, *Chem. Eng. Sci.* 52, 4659 **(1997)**.
9. M. Vanni, *J. Colloid Interface Sci.* 221, 143 **(2000)**.
10. A. Kalani and P. D. Christofides, *Comput. Chem. Eng.* 26, 1153 **(2002)**.
11. A. T. Suddah and T. M Mark, *Aerosol Science* 35, 889 **(2004)**.
12. D. W. Pepper and J. C. Heinrich, The Finite Element Method: Basic Concepts and Applications, Hemisphere Publishing Corporation, USA **(1992)**.
13. B. James and P. D. Christofides, *International Journal of Control* 73, 439 **(2000)**.
14. A. H. Aleck and A. K. Costas, *Journal of Chemical Engineering Science* 60, 4157 **(2005)**.
15. S. Hailian, J. F. Fraser and G. Martin, *Journal of Process Control* 17, 379 **(2007)**.
16. S. Dan, H. E. F. Nael, L. Mingheng, M. Prashant, and P. D. Christofides, *Chem. Eng. J.* 6, 268 **(2006)**.
17. D. Meimaroglou, A. I. Roussos, and C. Kiparissides, *Chem. Eng. Sci.* 61, 5620 **(2006)**.
18. C. A. Dorao and H. A. Jakobsen, *Comput. Chem. Eng.* 30, 535 **(2006)**.
19. C. A. Dorao and H. A. Jakobsen, *Chem. Eng. Sci.* 61, 7795 **(2006)**.
20. R. B. Diemer and S. H. Ehrman, *Journal of Powder Technology* 156, 129 **(2005)**.
21. J. C. Barret and N. A. Webb, *J. Aerosol Sci.* 29, 31 **(1998)**.
22. E. Banabalova, *Vacuum* 53, 174 **(2000)**.
23. L. M. Moropeng and A. Kolesnikov, *J. Comput. Theor. Nanosci.* 7, 1490 **(2010)**.
24. O. Sadiku and A. Kolesnikov, *J. Comput. Theor. Nanosci.* 7, 1 **(2010)**.
25. S. E. Pratsinis, *Journal of Collide Interface Science* 124, 416 **(1998)**.
26. A. Kalani and P. D. Christofides, *Chem. Eng. Sci.* 54, 2669 **(1999)**.

Received: 10 May 2010. Accepted: 4 October 2010.